

RESEARCH ARTICLE

Open Access



# Erythropoietin regulates osteoclast formation via up-regulating PPAR $\gamma$ expression

Xiao Liu<sup>1</sup>, Mengxue Zhou<sup>2</sup>, Yifan Wu<sup>1</sup>, Xiang Gao<sup>1</sup>, Lei Zhai<sup>3</sup>, Liang Liu<sup>1\*</sup> and Huan Geng<sup>1\*</sup> 

## Abstract

Erythropoietin (EPO), expressed in red blood progenitor cells, primarily regulates erythropoiesis by binding to its receptor. Besides anemia, recent studies have identified new therapeutic indications for EPO that are not connected to red blood cell formation. Elevated EPO levels harm bone homeostasis in adult organisms and are associated with increased osteoclast; however, the underlying molecular mechanisms remain unclear. This study demonstrated that EPO enhanced osteoclast differentiation and bone resorption in vitro. We showed that EPO promoted osteoclast formation by up-regulating PPAR $\gamma$  expression through activating the Jak2/ERK signaling pathway. Consistently, PPAR $\gamma$  antagonists rescued the hyperactivation of osteoclasts due to EPO, while PPAR $\gamma$  agonists reversed the EMP9-mediated decrease in osteoclast differentiation. Further, exposing female mice to EPO for two months led to a decrease in bone mass and increased osteoclast numbers. The present results suggested that EPO promotes osteoclastogenesis by regulating the Jak2/ERK/ PPAR $\gamma$  signaling pathway. From a clinical perspective, the risk of compromised bone health should be considered when using EPO to treat anemia in post-operative patients with intertrochanteric fractures of the femur, as it could significantly impact the patient's recovery and quality of life.

**Keywords** EPO, Bone remodeling, Trabecular, Osteoblast differentiation, Osteocyte

## Introduction

Erythropoietin (EPO) is a renal hormone the kidney produces that effectively promotes erythropoiesis. Clinically, recombinant EPO is used to treat anemia caused by chronic kidney disease, cancer, or chronic blood loss (Kaneko et al. 2022). Besides hematopoietic tissue, EPO can stimulate non-erythrocyte response mediated by the erythropoietin receptor (EPOR), which is also expressed

in other normal tissues, such as the brain and bone. Extensive research has been conducted over the past two decades to examine the impact of EPO on bone metabolism (Suresh et al. 2020a, b, c). While many studies have shown that exogenous administration of high doses of EPO induces bone loss in adult mice (Singbrant et al. 2011; Shiozawa et al. 2010; Rauner et al. 2016), there is limited data supporting a direct impact of EPO on bone metabolism. Therefore, the exact role of EPO in bone remodeling and its mechanism of action remains unclear.

The maintenance of bone mass depends on the dynamic balance between osteoblast-mediated bone formation and bone resorption by osteoclast-mediated bone resorption (Han et al. 2020). Osteoclasts are the primary, if not the only, cells responsible for bone resorption (Wu et al. 2017). These large multinucleated cells differentiate from monocyte/macrophage cell lines stimulated by macrophage colony-stimulating factor (M-CSF) and

\*Correspondence:

Liang Liu

llzju2014@163.com

Huan Geng

genghuan1989@zju.edu.cn

<sup>1</sup>Department of Orthopedics, The Second Affiliated Hospital, School of Medicine, Zhejiang University, Hangzhou 310058, China

<sup>2</sup>Key Laboratory of Tea Biology and Resource Utilization of Ministry of Agriculture, Tea Research Institute, Chinese Academy of Agricultural Sciences, Hangzhou 310008, China

<sup>3</sup>Meiao Dingcheng Clinic Limited Company, Tianjin 300000, China



© The Author(s) 2024. **Open Access** This article is licensed under a Creative Commons Attribution 4.0 International License, which permits use, sharing, adaptation, distribution and reproduction in any medium or format, as long as you give appropriate credit to the original author(s) and the source, provide a link to the Creative Commons licence, and indicate if changes were made. The images or other third party material in this article are included in the article's Creative Commons licence, unless indicated otherwise in a credit line to the material. If material is not included in the article's Creative Commons licence and your intended use is not permitted by statutory regulation or exceeds the permitted use, you will need to obtain permission directly from the copyright holder. To view a copy of this licence, visit <http://creativecommons.org/licenses/by/4.0/>.

receptor activator of NF- $\kappa$ B ligand (RANKL) (Murata et al. 2022). RANKL, expressed in osteocytes, bone marrow stromal cells and activated T cells, is a central positive regulator of osteoclast formation (Tsukasaki et al. 2020). When RANKL binds to its receptors, RANK, it activates several intracellular signaling pathways, such as NF- $\kappa$ B and MAPK-AP-1 signaling pathways. Activation of these signaling pathways converges to stimulate the expression and activates the function of transcription factors to drive the osteoclast differentiation program (Tsukasaki et al. 2020). Recently, Suresh et al. demonstrated that pre-osteoclasts express functional EPOR, and they found that mice with overexpressed EPO had reduced bone mass due to an increased number of osteoclasts. This suggests that EPO may reduce bone mass by directly promoting osteoclast differentiation. Nevertheless, the mechanisms by which EPO regulates osteoclast differentiation remain unknown.

In this study, we examined the effectiveness of EPO on the differentiation of osteoclasts induced by RANKL and osteoclastic bone resorption. Our results demonstrated that EPO could promote osteoclastogenesis. The molecular mechanisms underlying EPO's ability to promote osteoclast differentiation involve increased intracellular PPAR $\gamma$  expression. Furthermore, EPO increases PPAR $\gamma$  expression primarily by inactivating Jak2/ERK.

## Materials and methods

### Cell culture and differentiation into osteoclasts

Mature osteoclasts were generated from bone marrow macrophages (BMMs) as described previously (Geng et al. 2017). Briefly, primary bone marrow cells were isolated from the femora of 5-week-old C57BL/6 mice. We cultured primary bone marrow cells in the complete medium containing 50 ng/mL recombinant M-CSF (R&D Systems, Minneapolis, MN, USA) for 3 days. Adherent cells at this stage were considered M-CSF-dependent BMMs and used as osteoclast precursors (cells at day 0). For osteoclastogenesis, the resultant BMMs were plated in 48-well plates and cultured in osteoclastogenic medium that consisted of 30 ng/mL M-CSF and 50 ng/mL RANKL for 4 days. We identified osteoclasts by staining for tartrate-resistant acid phosphatase (TRAP) activity. The cells were fixed with 4% paraformaldehyde and stained using the TRAP staining kit (Sigma-Aldrich, 387 A-1KT) based on the instructions received from the manufacturers. The TRAP<sup>+</sup> multinucleated (>3 nuclei) cells were counted as osteoclasts. According to the experimental requirements, 20IU/ml EPO (Sunshine Pharmaceutical, Shenyang, China), 0.5 mg/ml EMP9 (MedChemExpress, Wuhan, China), 20  $\mu$ M TZD (Sigma, St. Louis, MO, USA), or 10  $\mu$ M GW9662 (Sigma, St. Louis, MO, USA) were added into the osteoclast differentiation process.

### Immunofluorescence staining

The cells were fixed in 4% formaldehyde for 15 min, then the membranes were broken with 0.1% Triton X-100 for 10 min. The cells were treated with a blocking buffer and then exposed to primary antibodies targeting EPOR or PPAR $\gamma$  at 4 °C overnight. Subsequently, the cells were incubated with secondary antibody-labeled fluorescent at room temperature for 1 h. The cell nuclei were stained with DAPI, and fluorescence images were acquired using confocal laser scanning microscopy (Smartproof 5, Carl Zeiss, Oberkochen, Germany).

### Western blotting

The cells were washed twice with PBS and lysed in an ice-cold RIPA Lysis Buffer (Beyotime, China) containing protease inhibitors (Beyotime, China) for 20 min to extract total protein. Then, the supernatant was collected and centrifuged for 10 min at 12,000 g and 4 °C to obtain the protein sample. An equal amount of protein (50  $\mu$ g) was mixed with sodium dodecyl sulfate-polyacrylamide gel electrophoresis (SDS-PAGE) loading buffer (Beyotime, China) and then heated at 95 °C for 5 min. Subsequently, the protein sample was separated using SDS-PAGE on 14% polyacrylamide gels and then transferred to polyvinylidene difluoride membranes. The membranes were blocked with 5% skim milk and then examined using specific primary antibodies against EPOR (ABclona; Catalog: A2917), phospho- (p-)Jak2, Jak2, p-ERK, ERK, GAPDH and PPAR $\gamma$  overnight at 4 °C, followed by incubation with corresponding secondary antibodies at room temperature for 1 h. Finally, immunoreactive bands were detected with ECL reagents. All antibodies were purchased from ABclona.

### Actin ring formation assay

BMMs were seeded in confocal dishes and incubated in a complete inducing medium containing M-CSF and RANKL for four days to form actin rings. Subsequently, the cells were washed twice with PBS and fixed in 3.7% paraformaldehyde for 15 min. The cells were washed with PBS three times. Then, the cells were stained with rhodamine-conjugated phalloidin (Cytoskeleton, Inc., Denver, CO, USA), while the cell nucleus was stained with DAPI (Sigma-Aldrich) for 10 min. The cells were photographed using a confocal laser scanning microscopy.

### Bone resorption assay

BMMs ( $2 \times 10^4$  cells/well) were cultured in Osteo Assay Surface 24-well plates (Corning, NY, USA) coated with a calcium phosphate substrate. BMMs incubated in complete inducing medium containing M-CSF and RANKL for 6 days. Subsequently, the cells were washed with 10% sodium hypochlorite and rinsed with water three times. The images were captured using an ordinary light

microscope. The percentage of the resorbed bone surface area was quantified using ImageJ software.

### RT-qPCR

The total RNA was extracted using TRIzol according to the instructions received from the manufacturer. Then, RT-qPCR was performed to evaluate the transcription of osteoclast-related genes, including *Acp5*, *Ctsk*, *Mmp9*, *Calcr*, *NFATc1*, and *c-fos* using a SYBR Green qPCR Master Mix Kit (Applied Biosystems, Foster City, CA, USA) according to the manufacturer's recommendations. The relative mRNA expression was normalized with GAPDH. The primers used in this experiment was as follows:

*Acp5*, forward 5'-CTGGAG TGCACGATGCCAGCGAC A-3' and reverse 5'-TCCGTGCTCGGCGATGGACCAG A-3';

*Ctsk* forward 5'-GATACTGGACACCCACTGGGA-3' and reverse 5'-CATTCTCAGACACAATCCAC-3';

*Mmp9*, forward 5'-GGAGCACGGCAACGGAGAAG-3' and reverse 5'-CCTGGTCATAGTTGGCTGTGGTG-3';

*Calcr*, forward 5'-ATTTTGCCACTGCCTTTCAG-3' and reverse 5'-ATTTTCTCTGGGTGCGCTAA-3';

*NFATc1*, forward 5'-TGTTCTTCCCTCCCGATGTC T-3' and reverse 5'-CCCGTTGCTTCCAGAAAATA-3';

*c-fos*, forward 5'-TTGCTGATGCTCTTACTGG-3' and reverse 5'-GGATTTGACTGGAGGTCTGC-3';

GAPDH, forward 5'-AAATGGTGAAGGTCGGTGT G-3' and reverse 5'-TGAAGGGGTCGTTGATGG-3'.

### Animal treatments

The Animal Welfare Committee in Zhejiang University School of Medicine approved all animal care activities. Female C57BL/6 mice were randomly divided into four groups with 5 mice in each group at 10–12 weeks of age: (a) PBS, (b) rhEPO, (c) rhEPO+GW9962, and (d) rhEPO+ZOL. The rhEPO was administered intravenously at a dose of 5000 IU/kg three times per week for 2 months. The same volume of PBS, GW9962 (1 mg/kg), and ZOL (2 mg/kg,) was given to the control and rhEPO+ZOL group. rhEPO was obtained from Sunshine Pharmaceutical (Shenyang, China) for patient care.

### Micro-computed tomography analysis

After mice were sacrificed, the femora (1 per mouse) were soaked in ethanol. We used a micro-CT (Analyze 12.0, PerkinElmer) to scan the femurs. We scanned the entire length of the femur at a pixel size of 15  $\mu$ m, and analyzed the results according to the manufacturer's instructions. Region-of-interest (ROI) was defined from 0.225 mm (15 image slices) to 2.475 mm (165 image slices), with the growth plate slice defined as 0 mm. We performed an analysis of bone-related parameters in the ROI region. We used 3D models to enhance the interpretation of the images by reconstructing the data specifically from the

ROI region. The software (Analyze 12.0, PerkinElmer) was used to analyze trabecular microstructural parameters, including bone mineral density (BMD), trabecular number (Tb. N), trabecular bone volume per tissue volume (BV/TV), trabecular thickness (Tb. Th) and trabecular separation (Tb. Sp).

### TRAP staining of tibias

After animal sacrifice, the tibias per mouse were fixed in 4% paraformaldehyde for 48 h. After the samples were decalcified in 0.5 M EDTA for 4 weeks, they were embedded in paraffin. Five-micrometers-thick sections of the tibias were performed the tartrate-resistant acid phosphatase (TRAP) staining using the standard protocol.

### ELISA Analysis and blood analysis

After the final dose of injection, blood was collected by enucleation of the eyeballs, and serum was collected by separation from the clotted blood for ELISA assay and blood analysis. 0.5 mL mouse whole blood was collected in a 2 mL centrifuge tube containing 2.5  $\mu$ L of 2% heparin sodium. Then, blood parameters (hematocrit, RBCs and hemoglobin) were measured using a Sysmex automated blood cell counter (Sysmex XE-2100 and XE-5000). 1mL mouse whole blood was collected in a 2 mL centrifuge tube. Serum was collected from the supernatant of centrifuged mouse whole blood. Then, bone metabolism level was evaluated by measuring the concentration of serum C-terminal telopeptides of type I collagen (CTX-1). Serum CTX-1 levels were analyzed using a mouse CTX-1 EIA kit (Immunodiagnostic Systems) according to the manufacturer's instructions.

### Statistical analysis

The data is presented as the mean  $\pm$  standard deviation (SD). Statistical analysis was performed using SPSS 20.0 (SPSS Science Inc., Chicago, Illinois). Statistical significance was assessed using a one-way analysis of variance (ANOVA) analysis. A significant difference was considered as a P value < 0.05.

## Results

### EPOR is expressed in BMMs

It is well known that EPO can induce hematopoiesis via EPOR expressed on erythroid progenitor cells. However, our results showed that EPOR was identified as being expressed on BMMs (Fig. 1A), which was consistent with the previous report (Lifshitz et al. 2010). Moreover, we observed a decrease in EPOR levels from the beginning of RANKL-induced osteoclastogenesis when M-CSF was present (Fig. 1B, C).

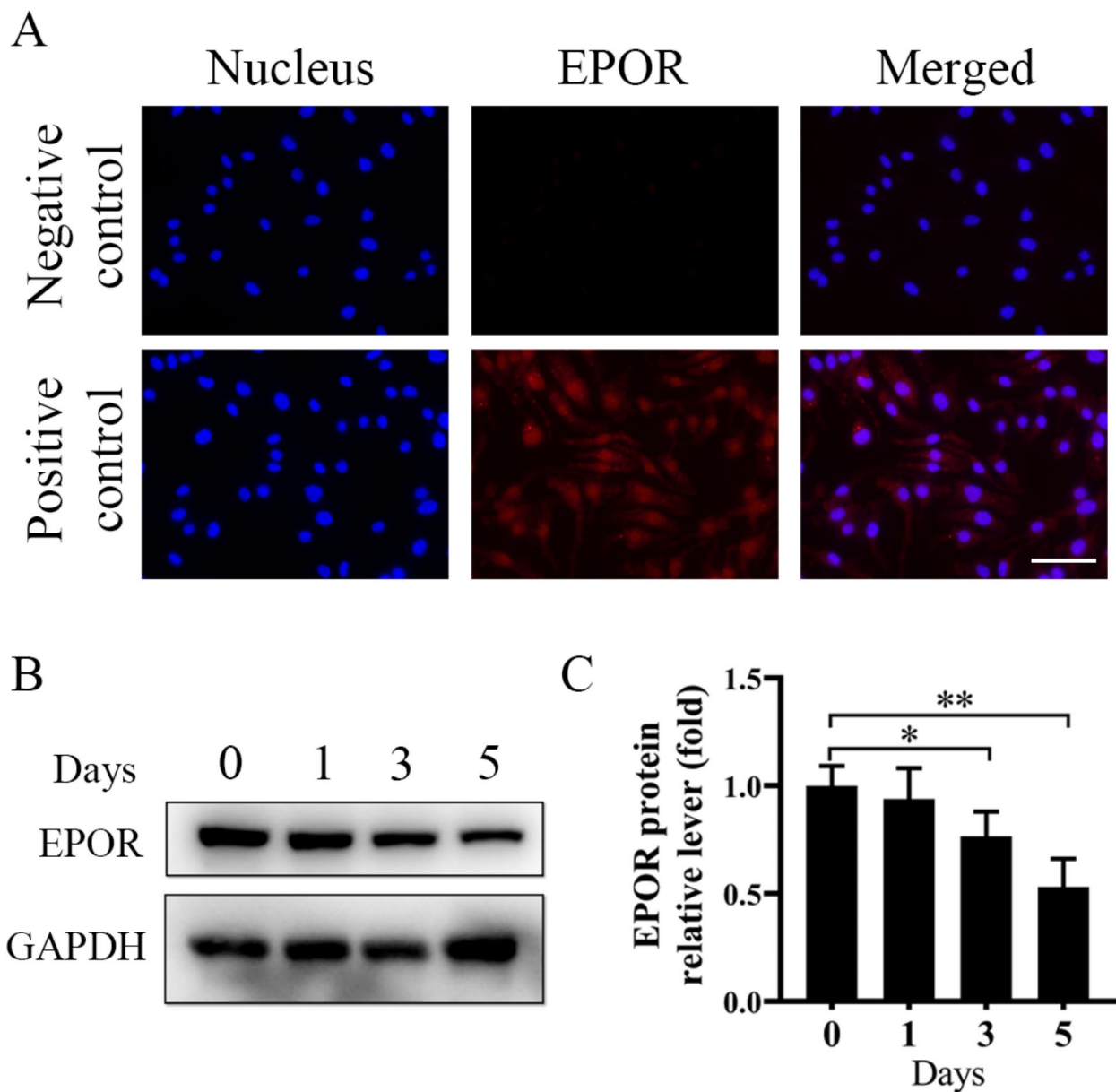


**Fig. 1** EPOR is expressed on BMMs. **(A)** Confocal analysis of EPOR (red) expression on BMMs. Scale bar = 100  $\mu$ m. **(B, C)** Western blots showing the expression of EPOR on 0, 1, 3, and 5 days after osteoclastic induction, and its quantification;  $n = 3$ . Error bars are mean  $\pm$  SD; \* $P < 0.05$ ; \*\* $P < 0.01$ ; NS, not significant

#### EPO promotes RANKL-induced osteoclast differentiation

Biologically, osteoclasts are commonly differentiated from BMMs under treatment with recombinant M-CSF and RANKL in vitro. The cells were treated with rhEPO, EMP9, or a combination during the differentiation of BMMs into osteoclasts. The results showed that rhEPO increased the area of TRAP<sup>+</sup> osteoclast and the relative cell size of TRAP<sup>+</sup> multinuclear osteoclast (nuclei > 3) after four days of incubation for cell differentiation as compared to the control (Fig. 2A, D, and E). Moreover, we found that EMP9 (an EPOR antagonist) (Luo et al.

2013) suppressed the EPO-enhanced osteoclast formation (Fig. 2A, D, and E; Figure S1). The formation of actin rings, a unique cytoskeletal structure found in mature osteoclasts that facilitates bone absorption (Geng et al. 2017), was also superior in rhEPO-treated cells compared to the control group, and EMP9 suppressed the EPO-enhanced actin ring formation (Fig. 2B, F). Furthermore, it was found to separately enhance the bone resorption activity of osteoclasts, which was also reversed by EMP9 (Fig. 2C, G). The data demonstrated that EPO/EPOR



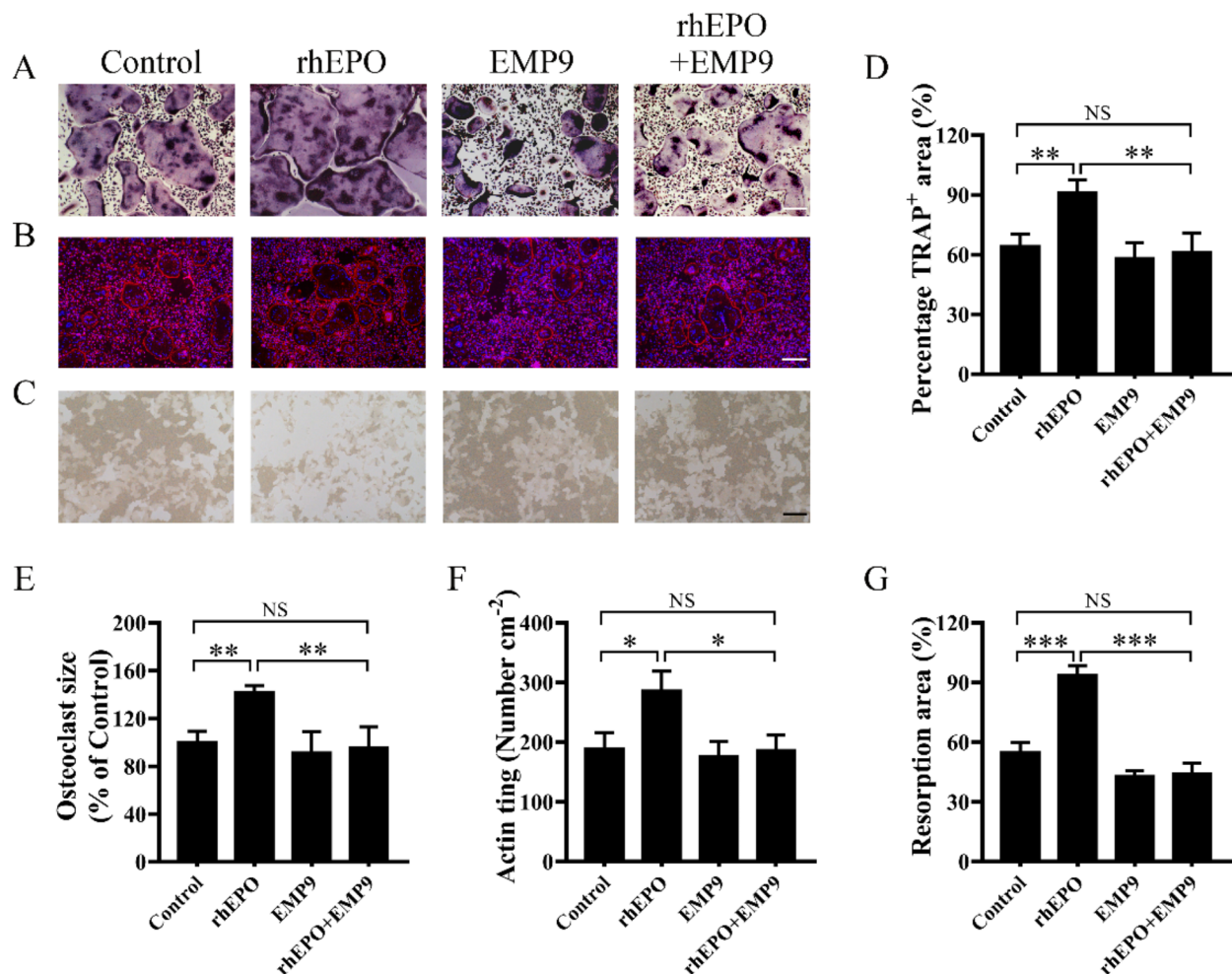


**Fig. 2** EPO enhances RANKL-induced osteoclast differentiation and bone resorption in vitro. **(A)** Representative TRAP staining images of BMMs treated with 30 ng/mL M-CSF and 50 ng/mL RANKL for four days in the presence of EPO and EMP9. Scale bar = 200  $\mu$ m. **(B)** Representative images of osteoclasts with actin ring (red) and cell nucleus (blue); the BMMs were treated with 30 ng/mL M-CSF and 50 ng/mL RANKL for four days in the presence of EPO or/and EMP9. Scale bar = 200  $\mu$ m. **(C)** Representative images of bone resorption pits on Corning Osteoassay 24-well plates. Scale bar = 200  $\mu$ m. **(D)** The area of TRAP<sup>+</sup> multinucleated cells (nuclei > 3) was quantified in each group. **(E)** The relative cell size of TRAP<sup>+</sup> multinuclear cells (nuclei > 3) was quantified in each group. **(F)** EPO increased the number of multinucleated cells (nuclei > 3) with actin rings. **(G)** The relative resorption area was quantified by using ImageJ Software. Error bars are mean  $\pm$  SD of triplicate experiments; \* $P$  < 0.05; \*\* $P$  < 0.01; \*\*\* $P$  < 0.001; NS, not significant

signaling in BMMs could enhance osteoclast differentiation and bone resorption in vitro.

#### EPO up-regulated osteoclastogenic gene expression

Mature osteoclasts express several specific genes that are vital for extracellular matrix degradation and bone resorption (Jacome-Galarza et al. 2019). Their gene products include TRAP, cathepsin K, matrix metalloproteinase-9, and calcitonin receptor (McDonald et al. 2021). Our results showed that EPO up-regulated the expression of these genes by approximately 120–150%, which was effectively inhibited by the EPOR antagonist EMP9 (Fig. 3A–D). RANKL binding to its receptor RANK initiates a complex signaling cascade that regulates lineage commitment and osteoclast differentiation (Shinohara et

al. 2008). It was reported that *c-fos* plays a crucial role in mediating osteoclast differentiation; mice that lack *c-fos* developed osteosclerosis due to impaired osteoclast differentiation (Grigoriadis et al. 1994). RANKL induces *c-fos* expression, which is required to induce the nuclear factor of activated T cells and cytoplasmic calcineurin-dependent-1 (NFATc1), a central transcription factor that governs osteoclast differentiation (Matsuo et al. 2000). Notably, EPO treatment significantly up-regulated the expression of *c-fos* and NFATc1, while this effect was abrogated by EMP9 (Fig. 3E, F).

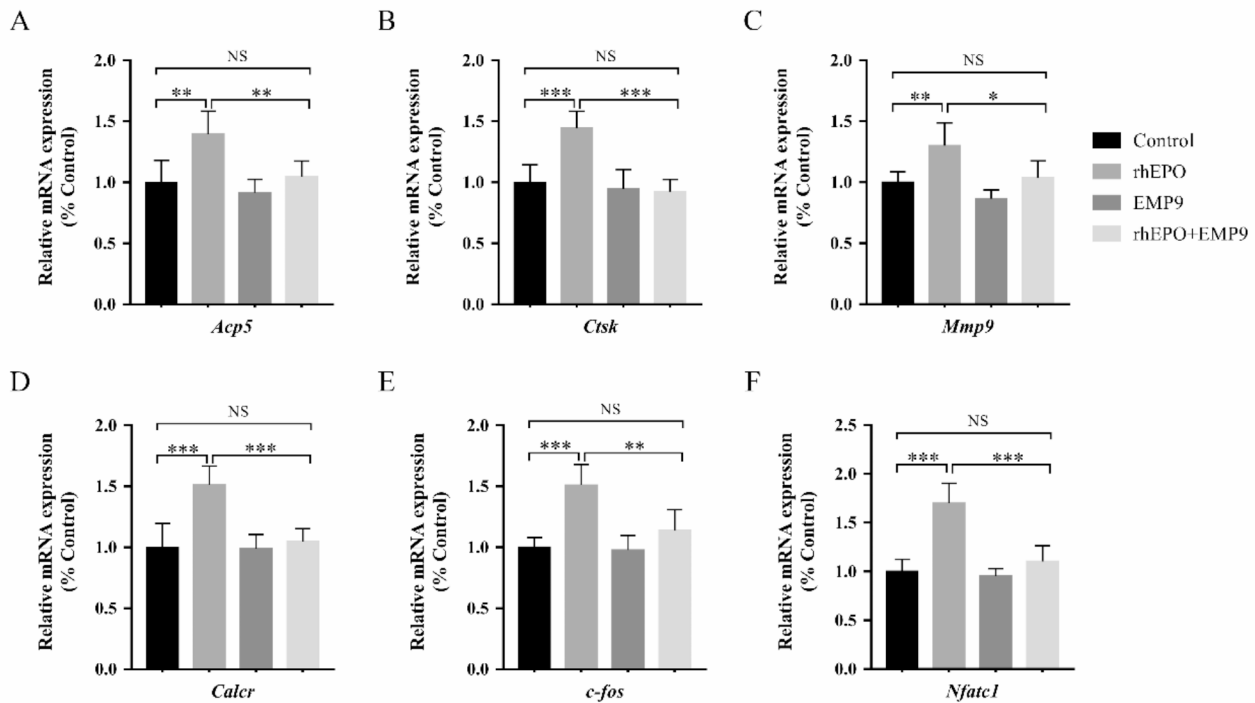


**Fig. 3** EPO up-regulated mRNA expression of RANKL-induced osteoclast-specific functional genes and transcription factors. EPO up-regulated osteoclast-specific functional genes (A) *Acp5*, (B) *Ctsk*, (C) *Mmp9*, (D) *Calcr*, and transcription factors (E) *c-fos*, (F) *Nfatc1* expression. Error bars are mean  $\pm$  SD of triplicate experiments; \* $P < 0.05$ ; \*\* $P < 0.01$ ; \*\*\* $P < 0.001$ ; NS, not significant

### EPO promotes PPAR $\gamma$ expression during osteoclast differentiation

We investigated the mechanisms involved in EPO/EPOR-mediated osteoclast differentiation. EPO binding to its receptor EPOR activates the STAT5, PI3K-AKT, and MEK-ERK, STAT5 pathways, inducing Jak2 phosphorylation (Nairz et al. 2012). Among these cascades, a previous study confirmed that the activation of ERK increased the PPAR $\gamma$  expression in macrophages (Luo et al. 2016). Moreover, PPAR $\gamma$  directly regulated the expression of *c-fos* to promote osteoclastogenesis (Wan et al. 2007). Therefore, we hypothesized that EPO might promote osteoclast differentiation via the Jak2-ERK-PPAR $\gamma$  pathway. Since EPO up-regulated the expression of transcription factors *c-fos* (Fig. 3E), we examined the expression of PPAR $\gamma$  in response to EPO treatment. The results showed that EPO increased the mRNA and protein amounts of PPAR $\gamma$  in a time-dependent manner during osteoclastogenesis (Fig. 4A, B). Moreover, the elevated expression of PPAR $\gamma$  protein by EPO could be reversed by EMP9 (Fig. 4C, D). Furthermore, the activation of Jak2 and ERK was induced by EPO in a time-dependent manner, while the total protein amounts of Jak2 and ERK were not influenced by EPO (Fig. 4E). The Jak2 inhibitor (AG490) attenuated EPO-induced PPAR $\gamma$  expression and the activation of Jak2 and ERK in BMMs (Figure S2B).

The ERK inhibitor (PD98059) decreased EPO-induced PPAR $\gamma$  expression and ERK activation but not Jak2 in BMMs (Figure S2B). The PPAR $\gamma$  siRNA suppressed the PPAR $\gamma$  expression but did not affect Jak2 and ERK in BMMs (Figure S2 A, B). The present data indicated that EPO promoted osteoclast differentiation via the Jak2-ERK-PPAR $\gamma$  cascade.

### EPO promoted RANKL-induced osteoclast differentiation through PPAR $\gamma$

PPAR $\gamma$  is important for osteoclastogenesis. Loss of function by targeted PPAR $\gamma$  deletion impairs osteoclast differentiation and bone resorption, resulting in osteopetrosis (Wan et al. 2007). GW9662 (a PPAR $\gamma$  antagonist) significantly suppressed EPO-promoted osteoclast differentiation. Moreover, thiazolidinediones (TZDs, a PPAR $\gamma$  agonist) could reverse the EMP9-mediated decrease in osteoclast differentiation (Fig. 5A-C). Furthermore, GW9662 suppressed EPO-induced mRNA expression of transcription factors *c-fos* and NAFATc1, and TZDs could reverse EMP9-mediated down-regulation of *c-fos* and NAFATc1 expression (Fig. 5D, F). These results indicated that EPO promotes osteoclast differentiation through PPAR $\gamma$ .

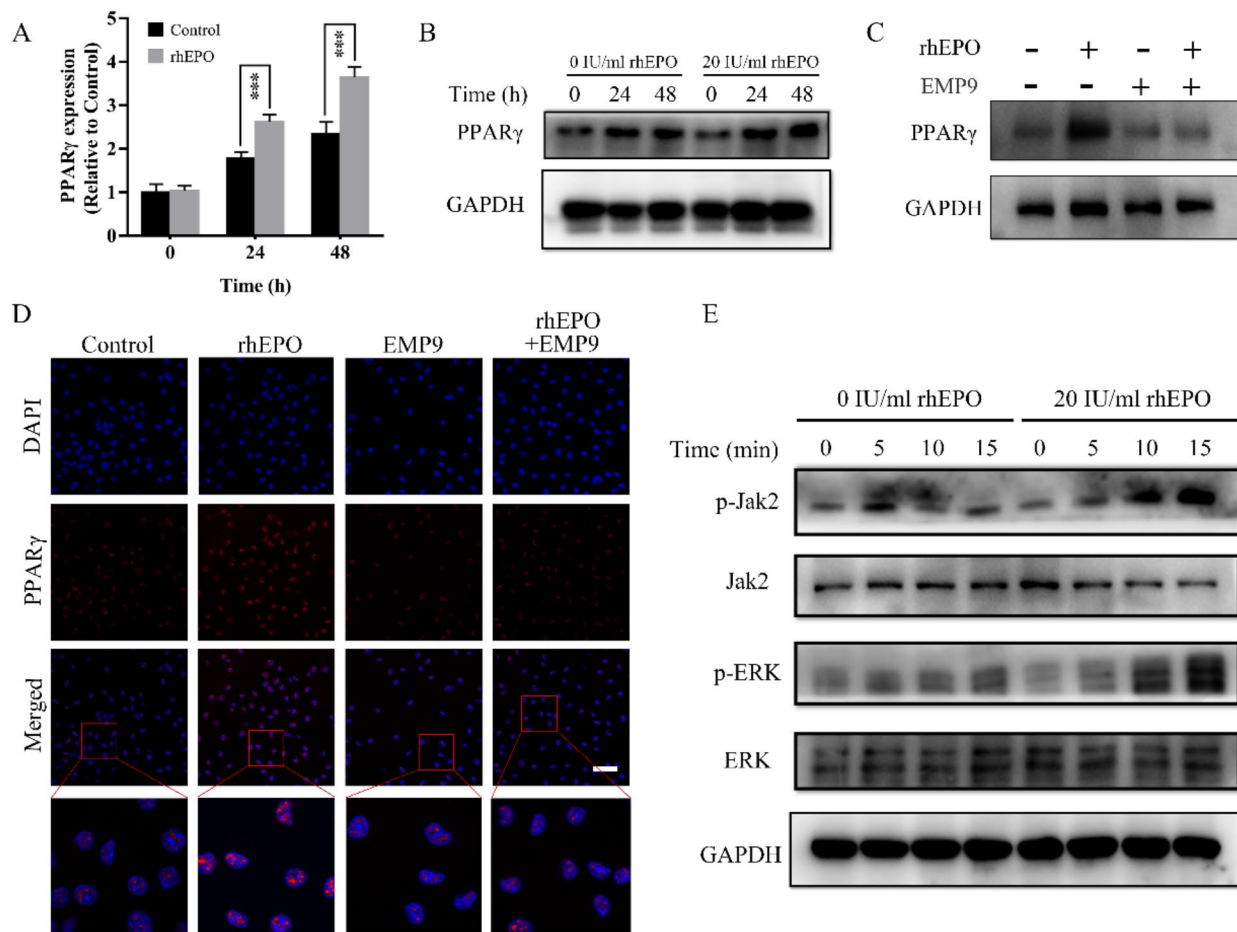


**Fig. 4** EPO induced PPAR $\gamma$  expression during osteoclast differentiation. **(A)** EPO up-regulated the transcription factor PPAR $\gamma$  mRNA expression at indicated time points. **(B)** EPO up-regulated the transcription factor PPAR $\gamma$  protein expression at indicated time points. **(C)** BMMs were incubated with 30 ng/mL M-CSF and 50 ng/mL RANKL in the presence of EPO or/and EMP9 for 24 h, and the PPAR $\gamma$  protein expression was measured using Western blot. **(D)** The PPAR $\gamma$  protein expression was measured using immunofluorescence after different treatments. **(E)** The phosphorylated (p-) and total Jak2 and ERK protein expression were measured after different treatments at indicated time points. Error bars are means  $\pm$  SD,  $n=3$ ; \* $P < 0.05$ ; \*\* $P < 0.01$ ; \*\*\* $P < 0.001$ ; NS, no significant

#### Epo induced trabecular bone loss in adult female mice

As EPO promotes osteoclast differentiation, we examined the effects of EPO on bone loss. We used micro-CT to quantify the bone density by analyzing various bone parameters. As previously reported, EPO significantly induced bone loss (Fig. 6A) (Hiram-Bab et al. 2015). Moreover, EPO significantly decreased bone mineral density (BMD), volume/total volume (BV/TV), trabecular number (Tb.N), and trabecular thickness (Tb.Th) (Fig. 6B-E), and increased trabecular separation (Tb.Sp) (Fig. 6F). After analyzing micro CT parameters, the BMD, BV/TV, Tb.N, Tb.Th, and Tb.Sp were all restored to the level of the control group with the injection of GW9662 and zoledronate (ZOL) (Fig. 6A-F). ZOL, the third-generation drug of bisphosphonates with strong bone affinity, has been employed to treat osteoporosis by inhibiting osteoclastogenesis. Then we used histological

TRAP staining to label osteoclasts in the bone trabecula region. EPO increases TRAP-positive staining in the trabecula region compared with the PBS group. However, GW9662 and ZOL reversed the effect of EPO on TRAP-positive staining (Fig. 6G, H). Finally, we evaluated bone metabolism level by measuring serum bone resorption marker C-terminal telopeptides of type I collagen (CTX-1) and bone formation marker procollagen type I N-terminal propeptide (PINP). As speculated, EPO significantly increased systemic bone resorption, which was also reversed by GW9662 and ZOL (Figure S3). EPO and ZOL did not affect bone formation levels. Moreover, EPO significantly increased the number of red blood cells, hemoglobin level and hematocrit compared with PBS group. EPO in combination with GW9662 and EPO with ZOL group exhibited red blood cell parameters similar to those of EPO group. (Figure S4).

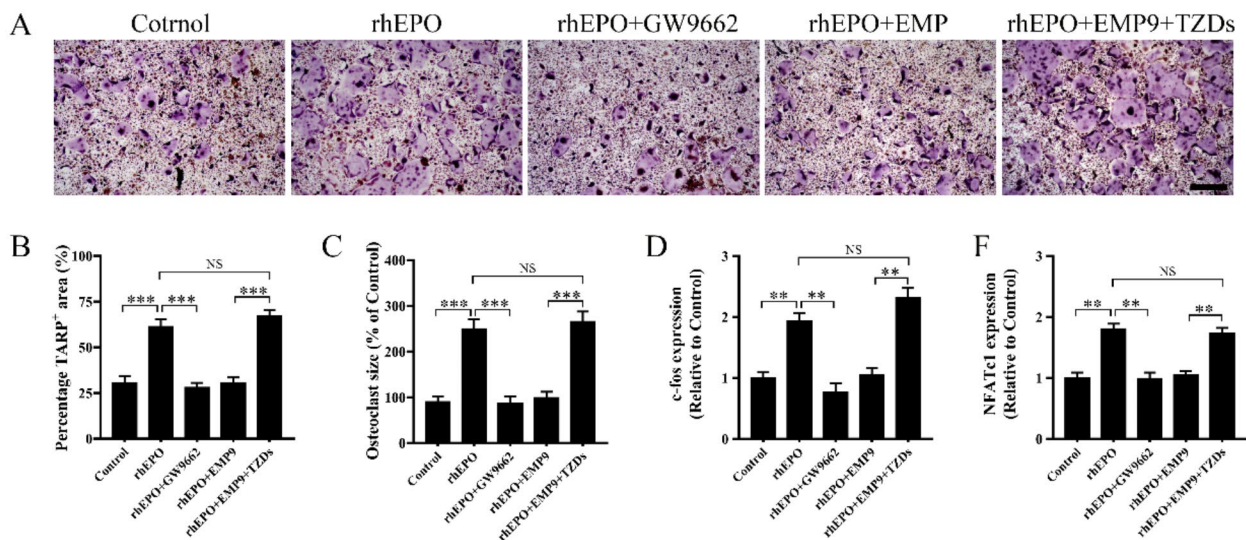


**Fig. 5** EPO enhanced osteoclast differentiation via inducing PPAR $\gamma$ . **(A)** Representative TRAP staining images of BMMs treated with 30 ng/mL M-CSF and 50 ng/mL RANKL for 4 days in the presence of EPO/EPO + GW9662/EPO + EMP9/EPO + EMP9 + TZDs. Scale bar = 200  $\mu$ m. **(B)** The area of TRAP<sup>+</sup> multinucleated cells (nuclei > 3) was quantified in each group. **(C)** The relative cell size of TRAP-positive multinuclear cells (nuclei > 3) was quantified in each group. **(D, E)** RT-qPCR was used to detect the mRNA expression of transcription factors **(D)** *c-fos* and **(F)** *Nfatc1*. Error bars are mean  $\pm$  SD of triplicate experiments; \*\* $P$  < 0.01; \*\*\* $P$  < 0.001; NS, no significant

## Discussion

Researchers showed that the administration of high doses of EPO to adult mice induces bone loss (Rauner et al. 2016; Suresh et al. 2020a, b, c). EPO can induce bone loss by increasing bone resorption by osteoclasts and decreasing bone formation by osteoblasts. Notably, excessive or overactive osteoclasts are the primary reason for bone loss in disorders like osteoporosis and Paget's disease is the presence of excessive or overactive osteoclast (Kim et al. 2021). Therefore, a viable strategy for treating these diseases is to focus on inhibiting the differentiation and activity of osteoclasts. This study demonstrated that EPO promoted osteoclastogenesis and bone resorption in vitro and in vivo. The molecular mechanism by which EPO/EPOR stimulates osteoclastogenesis is the regulation of downstream PPAR $\gamma$ .

Suresh et al. previously reported that EPOR is expressed in nonerythroid cells (Suresh et al. 2019). Our results showed that EPOR is also expressed in BMMs (Fig. 1A). However, we observed decreased EPOR expression from initiating RANKL-induced osteoclastogenesis in the presence of M-CSF (Fig. 1B, C), suggesting that RANKL signaling may down-regulate EPOR during osteoclastogenesis. Functional EPOR is expressed by several non-erythroid cells, indicating that EPO may have a broad regulatory role beyond erythropoiesis (Suresh et al. 2020a, b, c). In this study, we specifically evaluated the effect of EPO/EPOR signaling on osteoclast differentiation and observed that EPO increased both osteoclast formation and bone resorption ability. These findings

are consistent with the study by Hiram-Bab et al., which demonstrated that even a low dose of EPO stimulated osteoclastogenesis (Hiram-Bab et al. 2017; Kim et al. 2012). However, Singbrant et al. reported both EPO and erythroblasts did not stimulate osteoclast differentiation in cocultures of BMMs and calvarial osteoblasts (Singbrant et al. 2011). We speculated that this may be because EPO inhibits the formation of osteoblast, thus weakening the coupling between osteoblast and osteoclast. Other studies supported that EPO can promote osteoclast differentiation, consistent with our findings (Shiozawa et al. 2010; Li et al. 2015).

However, the mechanism by which EPO promotes osteoclast differentiation is unclear. Although EPO is well-known for its ability to promote erythropoiesis, recent studies have found that EPO has extrahematopoietic properties via EPORs expressed in nonhematopoietic tissues. For instance, rhEPO activates the PI3K/Akt to upregulate PPAR $\gamma$ , enhance the cellular antioxidant capacity, and protect neurons in rats subjected to oxidative stress (Wang et al. 2022). Furthermore, Ge et al. found that EPO/EPOR signaling activates the hepatic AKT pathway by increasing PPAR $\gamma$  expression and activity, which improves hepatic insulin resistance (Ge et al. 2015).

Biologically, osteoclasts are derived from the monocyte/macrophage lineage in response to RANKL (Bae et al. 2023). RANKL binding to RANK sequentially activates the downstream signaling pathways, ultimately inducing the expression and activation of *c-fos* and



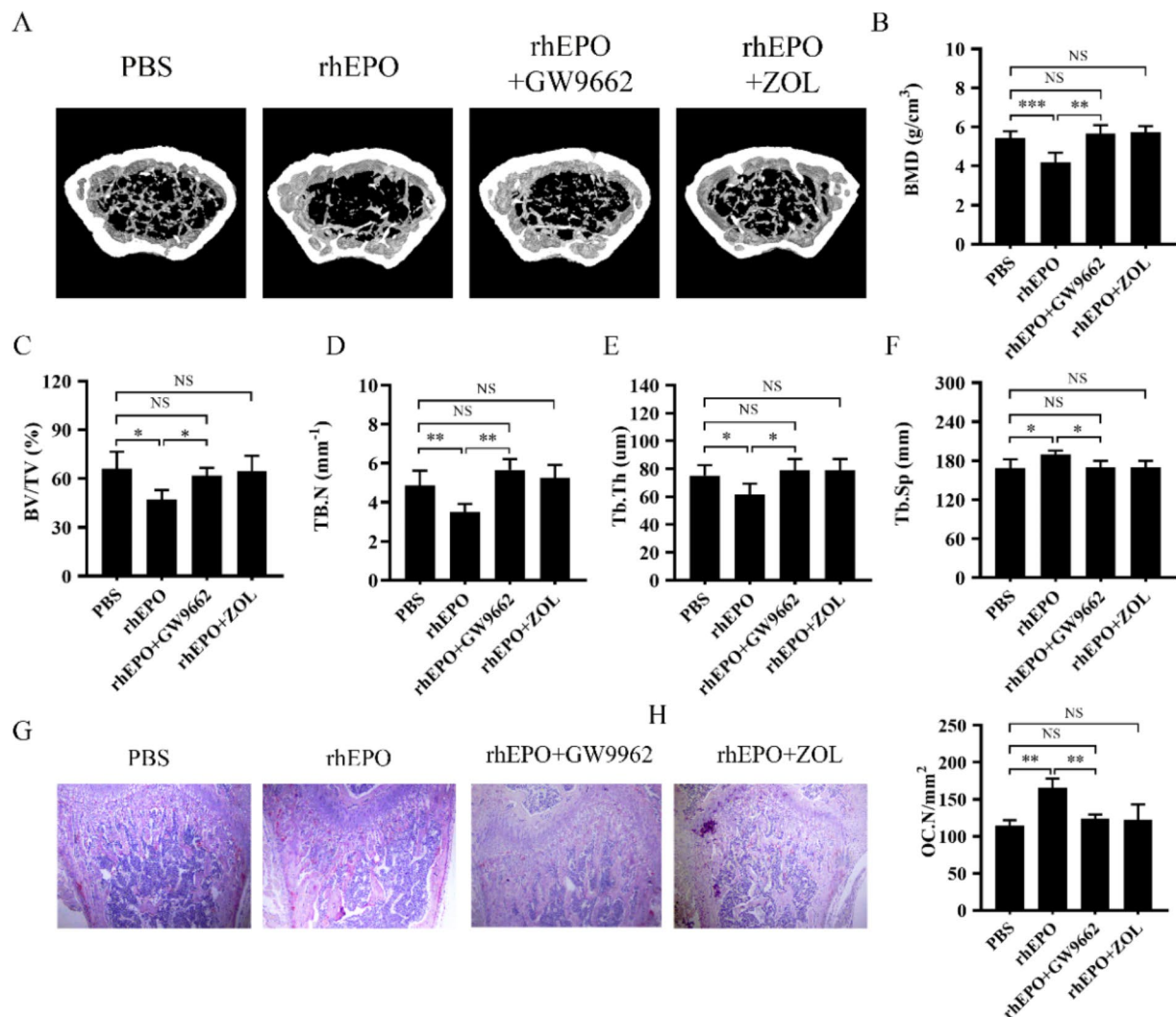


**Fig. 6** EPO increased bone loss in vivo. **(A)** Representative micro-CT images of mouse distal femur. **(B–F)** Quantitative micro-CT analysis of BMD, BV/TV, Tb.N, Tb.Th and Tb.Sp. **(G)** Light micrographs of TRAP-staining of decalcified bones. Scale bar = 200  $\mu$ m. **(H)** Quantification of osteoclast number (Oc.N) in G. Error bars are means  $\pm$  SD,  $n = 5$ ; \* $P < 0.05$ ; \*\* $P < 0.01$ ; \*\*\* $P < 0.001$ ; NS, no significant

NFATc1, with two key transcription factors that drive osteoclast differentiation (Murata et al. 2022). In addition, EPO binding to its receptor EPOR activates the phosphorylation of Jak2 to activate MEK-ERK. This activation of ERK then increases the PPAR $\gamma$  expression in macrophages, which aids in the clearance of dying cells (Luo et al. 2016). Our results showed that EPO activated the phosphorylation of Jak2 and ERK in a time-dependent manner. Furthermore, EPO increased the expression of PPAR $\gamma$  in the downstream of JAK-ERK during osteoclastogenesis (Fig. 4G, F). Previous studies showed that PPAR $\gamma$  directly regulated the expression of c-fos to promote osteoclastogenesis (Wan et al. 2007; Wei et al. 2010). As c-fos is a crucial mediator in osteoclast formation, required for the induction of NFATc1 nuclear factor, mice lacking c-fos develop osteosclerosis due to the

obstruction of osteoclast differentiation (Wada et al. 2006). Our results showed that EPO up-regulated the expression of transcription factors c-fos and NFATc1. Furthermore, GW9662 significantly suppressed EPO-promoted osteoclast differentiation by inhibiting the expression of transcription factors c-fos. Therefore, it is apparent that EPO functions through PPAR $\gamma$  to promote osteoclast differentiation.

Finally, we showed that exposure to EPO in adult mice resulted in bone loss, which was found to be associated with EPO-stimulated osteoclastogenesis. However, bone loss induced by EPO was reversed by ZOL. This finding is clinically significant as EPO is frequently used to treat anemia in postoperative patients with intertrochanteric fractures of the femur. As EPO treatment leads to bone

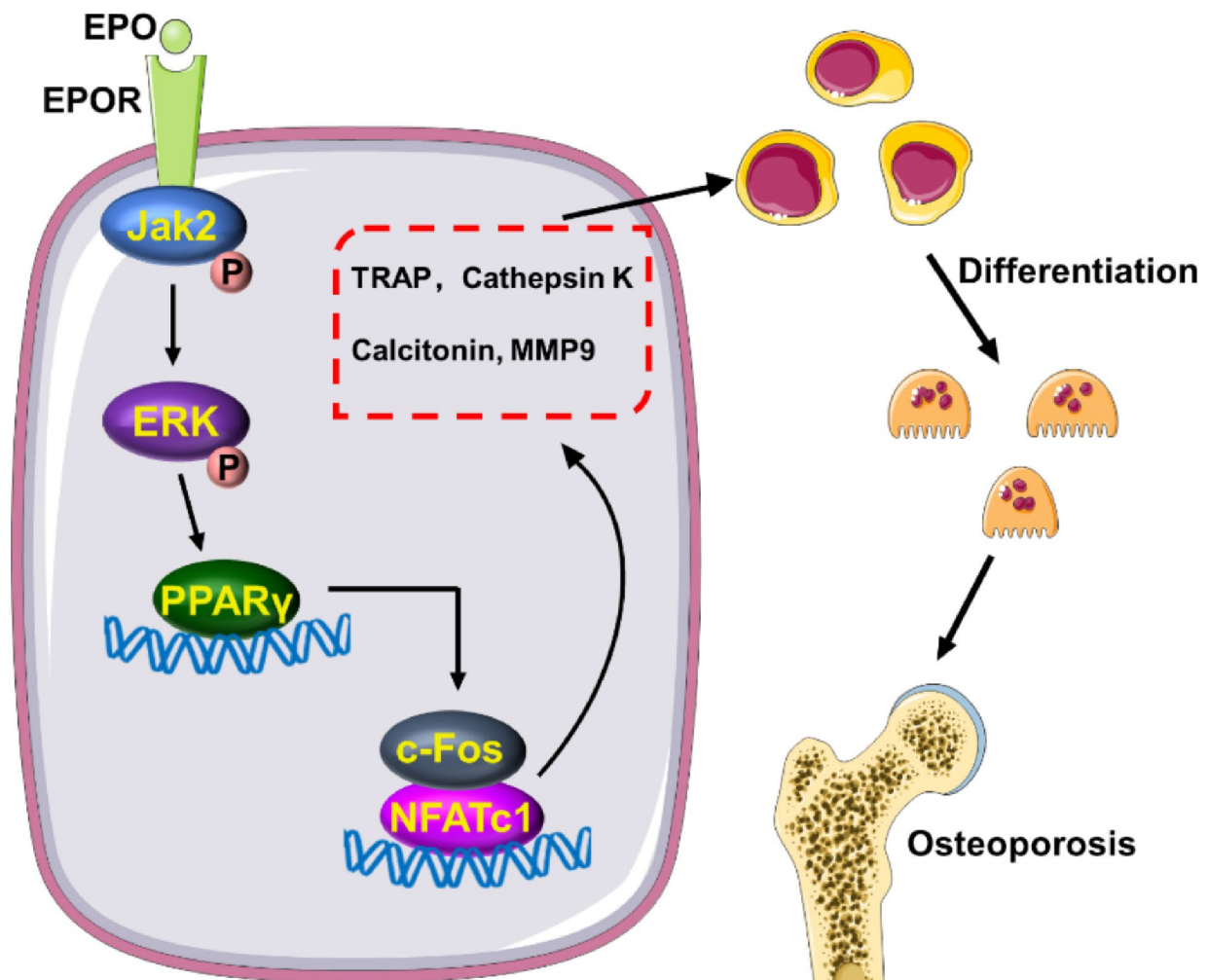


**Fig. 7** EPO binding to its receptor EPOR activates the Jak2/ERK signal pathway, increasing PPAR $\gamma$  expression. Then, PPAR $\gamma$  directly regulated the expression of c-fos to promote osteoclast differentiation and enhanced osteoclastic bone resorption

loss, these patients may benefit from antiosteoporosis drugs such as denosumab and ZOL.

### Conclusion

This study confirmed that EPO promoted RANKL-induced osteoclast differentiation and enhanced osteoclastic bone resorption. The underlying mechanism is related to the activation of the Jak2/ERK signal pathway, leading to an increased PPAR $\gamma$  expression (Fig. 7). Clinically, the risk of bone loss should be considered when using EPO to treat anemia.

### Supplementary Information

The online version contains supplementary material available at <https://doi.org/10.1186/s10020-024-00931-7>.

Supplementary Material 1

Supplementary Material 2

### Acknowledgements

This work benefited from discussions with Dr. Yiyi Qi.

### Author contributions

Xiao Liu: Methodology, Validation, Investigation, Writing – original draft, Writing – review & editing. Mengxue Zhou: Investigation, Validation, Writing – review & editing. Yifan Wu: Investigation, Writing – review & editing. Lei zhai: Investigation, Writing – review & editing. Liang Liu: Conceptualization, Validation, Writing – review & editing, Supervision. Huan Geng: Conceptualization, Methodology, Validation, Investigation, Resources, Data curation, Writing – original draft, Writing – review & editing, Supervision, Project administration.

### Funding

Financial support from the Natural Science Foundation of Zhejiang Province, Y21H070011, is acknowledged.

### Data availability

The original contributions presented in the study are included in the article; further inquiries can be directed to the corresponding authors.

## Declarations

### Ethics approval and consent to participate

All animal care was approved by the Animal Welfare Committee in Zhejiang University School of Medicine (AIRB-2022-0510).

### Consent for publication

Not applicable.

### Competing interests

The authors declare that they have no known competing financial interests or personal relationships that could have appeared to influence the work reported in this paper.

Received: 27 April 2024 / Accepted: 6 September 2024

Published online: 15 September 2024

## References

- Bae S, Kim K, Kang K, et al. RANKL-responsive epigenetic mechanism reprograms macrophages into bone-resorbing osteoclasts. *Cell Mol Immunol*. 2023;20:94–109.
- Ge Z, Zhang P, Hong T, et al. Erythropoietin alleviates hepatic insulin resistance via PPAR $\gamma$ -dependent AKT activation. *Sci Rep*. 2015;5:17878.
- Geng H, Chang YN, Bai X, et al. Fullerene nanoparticles suppress RANKL-induced osteoclastogenesis by inhibiting differentiation and maturation. *Nanoscale*. 2017;9:12516–23.
- Grigoriadis AE, Wang ZQ, Cecchini MG, et al. c-Fos: a key regulator of osteoclast-macrophage lineage determination and bone remodeling. *Science*. 1994;266:443–8.
- Han B, Geng H, Liu L, et al. GSH attenuates RANKL-induced osteoclast formation in vitro and LPS-induced bone loss in vivo. *Biomed Pharmacother*. 2020;128:110305.
- Hiram-Bab S, Liron T, Deshet-Unger N, et al. Erythropoietin directly stimulates osteoclast precursors and induces bone loss. *Faseb j*. 2015;29:1890–900.
- Hiram-Bab S, Neumann D, Gabet Y. Context-dependent skeletal effects of Erythropoietin. *Vitam Horm*. 2017;105:161–79.
- Jacome-Galarza CE, Percin GI, Muller JT, et al. Developmental origin, functional maintenance and genetic rescue of osteoclasts. *Nature*. 2019;568:541–5.
- Kaneko K, Sato Y, Uchino E, et al. Lineage tracing analysis defines erythropoietin-producing cells as a distinct subpopulation of resident fibroblasts with unique behaviors. *Kidney Int*. 2022;102:280–92.
- Kim J, Jung Y, Sun H, et al. Erythropoietin mediated bone formation is regulated by mTOR signaling. *J Cell Biochem*. 2012;113:220–8.
- Kim H, Lee K, Kim JM, et al. Selenoprotein W ensures physiological bone remodeling by preventing hyperactivity of osteoclasts. *Nat Commun*. 2021;12:2258.
- Li C, Shi C, Kim J, et al. Erythropoietin promotes bone formation through EphrinB2/EphB4 signaling. *J Dent Res*. 2015;94:455–63.
- Lifshitz L, Tabak G, Gassmann M, et al. Macrophages as novel target cells for erythropoietin. *Haematologica*. 2010;95:1823–31.
- Luo B, Jiang M, Yang X, et al. Erythropoietin is a hypoxia inducible factor-induced protective molecule in experimental autoimmune neuritis. *Biochim Biophys Acta*. 2013;1832:1260–70.
- Luo B, Gan W, Liu Z, et al. Erythropoietin Signaling in Macrophages promotes dying cell clearance and Immune Tolerance. *Immunity*. 2016;44:287–302.
- Matsuo K, Owens JM, Tonko M, et al. Fos1 is a transcriptional target of c-Fos during osteoclast differentiation. *Nat Genet*. 2000;24:184–7.
- McDonald MM, Khoo WH, Ng PY, et al. Osteoclasts recycle via osteomorphs during RANKL-stimulated bone resorption. *Cell*. 2021;184:1940.
- Murata K, Fang C, Terao C, et al. Hypoxia-sensitive COMMD1 integrates Signaling and Cellular Metabolism in Human macrophages and suppresses Osteoclastogenesis. *Immunity*. 2022;55:2209.
- Nairz M, Sonnweber T, Schroll A, et al. The pleiotropic effects of erythropoietin in infection and inflammation. *Microbes Infect*. 2012;14:238–46.
- Rauner M, Franke K, Murray M, et al. Increased EPO levels are Associated with Bone loss in mice lacking PHD2 in EPO-Producing cells. *J Bone Min Res*. 2016;31:1877–87.
- Shinohara M, Koga T, Okamoto K, et al. Tyrosine kinases Btk and Tec regulate osteoclast differentiation by linking RANK and ITAM signals. *Cell*. 2008;132:794–806.
- Shiozawa Y, Jung Y, Ziegler AM, et al. Erythropoietin couples hematopoiesis with bone formation. *PLoS ONE*. 2010;5:e10853.
- Singbrant S, Russell MR, Jovic T, et al. Erythropoietin couples erythropoiesis, B-lymphopoiesis, and bone homeostasis within the bone marrow microenvironment. *Blood*. 2011;117:5631–42.
- Suresh S, de Castro LF, Dey S, et al. Erythropoietin modulates bone marrow stromal cell differentiation. *Bone Res*. 2019;7:21.
- Suresh S, Lee J, Noguchi CT. Effects of Erythropoietin in White Adipose tissue and bone microenvironment. *Front Cell Dev Biol*. 2020a;8:584696.
- Suresh S, Alvarez JC, Dey S et al. Erythropoietin-Induced Changes in Bone and Bone Marrow in Mouse models of Diet-Induced obesity. *Int J Mol Sci* 2020b, 21.
- Suresh S, Lee J, Noguchi CT. Erythropoietin signaling in osteoblasts is required for normal bone formation and for bone loss during erythropoietin-stimulated erythropoiesis. *Faseb j*. 2020c;34:11685–97.
- Tsukasaki M, Huynh NC, Okamoto K, et al. Stepwise cell fate decision pathways during osteoclastogenesis at single-cell resolution. *Nat Metab*. 2020;2:1382–90.
- Wada T, Nakashima T, Hiroshi N, et al. RANKL-RANK signaling in osteoclastogenesis and bone disease. *Trends Mol Med*. 2006;12:17–25.
- Wan Y, Chong LW, Evans RM. PPAR-gamma regulates osteoclastogenesis in mice. *Nat Med*. 2007;13:1496–503.
- Wang H, Chen M, Zhang T, et al. Recombinant human erythropoietin upregulates PPAR $\gamma$  through the PI3K/Akt pathway to protect neurons in rats subjected to oxidative stress. *Eur J Neurosci*. 2022;56:4045–59.
- Wei W, Wang X, Yang M, et al. PGC1 $\beta$  mediates PPAR $\gamma$  activation of osteoclastogenesis and rosiglitazone-induced bone loss. *Cell Metab*. 2010;11:503–16.
- Wu M, Chen W, Lu Y, et al. Ga13 negatively controls osteoclastogenesis through inhibition of the Akt-GSK3 $\beta$ -NFATc1 signalling pathway. *Nat Commun*. 2017;8:13700.

## Publisher's note

Springer Nature remains neutral with regard to jurisdictional claims in published maps and institutional affiliations.